ISSN 1027-5495. Functional Materials, 26, No.2 (2019), p. 276-283.
doi:https://doi.org/10.15407/fm26.02.276

Optimization of preparation and removal of 4-nitrophenol from activated carbon loaded nano-iron by response surface methodology

***Zhang Jiankun*[1,2,3], *Feng Qiyan*[1], *Gao Mingxia*[2], *Zhang Linjun*[2], *Liu Jiaqiang*[2], *Zhang Xueyang*[2]**

[1]School of Environment Science and Spatial Informatics, China University of Mining and Technology, 21008 Xuzhou, China
[2]School of Environmental Engineering, Xuzhou University of Technology, 221111 Xuzhou, China
[3]Key Laboratory of Jiangxi Province for Persistant Pollutants Control and Resources Recycle, 330063 Nanchang, China

Received April 18, 2019

Taking 4-nitrophenol as the target pollutant, activated carbon-supported nano-iron materials were prepared by liquid phase reduction method. Taking $FeSO_4$, concentration, $NaBH_4$ concentration and the dosage of activated carbon as influencing factors, Box-Behnken response surface method was used to carry out three-factor and three-level experiments, and the preparation method of activated carbon-supported nano-iron materials was optimized. The results show that the interaction between $FeSO_4$ concentration and $NaBH_4$ concentration has a significant effect on the preparation of nano-iron materials, which plays a key role in the removal of 4-nitrophenol, and the effect of $FeSO_4$ concentration is more significant. The interaction between the dosage of activated carbon and $NaBH_4$ concentration is significant. The best preparation conditions of activated carbon loaded nano-iron are 2.334 g of $FeSO_4$ solution 100 mL, 0.462 mol/L of $NaBH_4$ solution 50mL, and the dosage of activated carbon 5.182 g. Under these conditions, the removal rate of the prepared nano-iron material can reach 98.2 % after treating 4-nitrophenol for 3 h, and the XRD pattern shows the characteristic diffraction absorption peak of Fe^0 at $2\theta = 42 - 44°$. After loading nano-iron, the specific surface area of activated carbon decreased 154.27 m^2/g, and the pore diameter decreased from 2.35 nm before loading to 2.26 nm after loading.

Keywords: activated carbon, nano-iron, 4-nitrophenol, response surface method.

Наночастицы железа на носителе с активированным углем получали методом жидкофазного восстановления с использованием в качестве примеси 4-нитрофенол. Для проведения трехфакторных и трехуровневых экспериментов использован метод Бокса-Бенкена. $FeSO_4$, $NaBH_4$ и активированный уголь выбрали в качестве влияющих факторов, что позволило оптимизировать метод приготовления наноразмерных материалов на основе активированного угля. Результаты показывают, что концентрации $FeSO_4$ и $NaBH_4$ играют ключевую роль в удалении 4-нитрофенола, при этом влияние концентрации $FeSO_4$ является более значительным. Установлены оптимальные условия приготовления наночастиц железа с активированным углем. Удаление загрязнителя может достигать 98,2 %. Рентгенограмма полученного материала показывает характерный пик дифракционного поглощения Fe^0 при $2\theta = 42 - 44°$. После загрузки наночастиц железа удельная площадь поверхности активированного угля уменьшилась до 154.27 $м^2/г$, а диаметр пор уменьшился с 2.35 нм до 2.26 нм.

Оптимізація синтезу і видалення 4-нітрофенолу з активованого вугілля, навантаженого наночастинками заліза, з використанням методології поверхні відповіді. *Чжан Цзянькунь, Фэн Циянь, Гао Минся, Чжан Линцзюнь, Лю Цзяцян, Чжан Сюян.*

Наночастки заліза на носії з активованим вугіллям отримано методом рідкофазного відновлення з використанням в якості домішки 4-нітрофенол. Для проведення трехфакторной і трьохповерхових експериментів використаний метод Бокса-Бенк. $FeSO_4$, $NaBH_4$ і активоване вугілля вибрано в якості факторів, що впливають, що дозволило оптимізувати метод приготування нанорозмірних матеріалів на основі активованого вугілля. Результати показують, що концентрації $FeSO_4$ і $NaBH_4$ грають ключову роль у видаленні 4-нітрофенолу, при цьому вплив концентрації $FeSO_4$ є більш значним. Встановлено оптимальні умови приготування наночастинок заліза з активованим вугіллям. Видалення забруднювача може досягати 98,2%. Рентгенограма отриманого матеріалу показує характерний пік дифракційного поглинання Fe0 при 2θ = 42-44°. Після завантаження наночастинок заліза питома площа поверхні активованого вугілля зменшилася до 154.2 м^2/г, а діаметр пір зменшився з 2.35 нм (до завантаження) до 2.26 нм (після завантаження).

1. Introduction

Nano-iron has many advantages, such as small scale, large surface effect, strong reduction ability, etc. It is widely used to remove [1, 2] refractory organic pollutants. However, nano-iron is easily oxidized and agglomerated in air. At the same time, nano-iron particles are fine, easy to lose, difficult to recycle and reuse. Therefore, in order to improve the dispersibility of nano-iron and reduce its agglomeration and oxidation, nano-iron can be loaded on carriers such as silica, zeolite, activated carbon, bentonite, resin, etc. [3, 4], which can not only maintain the inherent characteristics of nano-materials, but also enhance its stability and recovery rate, and is also suitable for reactor operation [5]. However, the loading technology of nano-iron has become an important issue in its practical application. Activated carbon is widely used as a loading material for nano-materials because of its large specific surface area, strong adsorption capacity and cheap and easily available raw materials. Activated carbon loaded with nano-iron not only has excellent adsorption of activated carbon and strong reduction of nano-iron [6–8]. Therefore, in this study, 4-nitrophenol is taken as the target pollutant, activated carbon is taken as the carrier, $FeSO_4$ concentration, concentration and the dosage of activated carbon are taken as the influencing factors, Box-Behnken response surface method is applied to carry out a three-factor and three-level experiment to optimize the preparation method of nano-iron material with activated carbon as the carrier, and provide certain reference for its application.

2. Experimental

2.1 Materials

Sodium borohydride ($NaBH_4$), ferrous sulfate heptahydrate ($FeSO_4{\cdot}7H_2O$), granular activated carbon, concentrated sulfuric acid, hydrochloric acid, polyethylene glycol, anhydrous ethanol and acetone are all analytically pure, and the experimental water is deionized water.

2.2 Preparation of activated carbon supported nano-iron

Granular activated carbon was soaked in 1 mol/L hydrochloric acid for 24 h, then washed with deionized water for many times, then soaked in anhydrous ethanol for 12 h, and dried by blowing at 105°C for 12 h. 2.5 g polyethylene glycol is weighed and dissolved in 40 mL absolute ethyl alcohol, then a certain amount of $FeSO_4{\cdot}7H_2O$ is weighed and dissolved in 60 mL deionized water, added into a three-necked flask in sequence, finally a certain amount of activated carbon is added and mixed evenly, and nitrogen is introduced to remove dissolved oxygen before the reaction. Slowly add 0.45 mol/L solution through a peristaltic pump, and continuously introduce nitrogen. After stirring for 1 hour through an electric stirrer, clean it with oxygen-free water for 3 times, then with anhydrous ethanol for 1 time, finally with acetone for 3 times. Dry and cool it in a vacuum drying oven at 70°C to obtain black powder, namely activated carbon loaded nano-iron, and store it in a brown vial filled with nitrogen in advance.

2.3. Characterization of activated carbon loaded with nano-iron

The XPert PRO MPD XRD analyzer was used to measure the activated carbon loaded nano-iron samples under the following conditions: X-ray tube voltage of 40 kV, current of 40 mA, 2θ range of 5° – 100°, and scanning speed of 10°/min. The functional groups on the surface of the sample crystal were determined by Nicolet IS10 Fourier infrared spectrometer. The specific surface area and pore diameter of the material were measured by KUBO-X1000 specific surface area and pore diameter analyzer. ESCALLAB250Xi X-ray photoelectron spectroscopy was used to analyze the elements and valence states in the materials.

2.4 Experimental methods

According to Box-Behnken's central composite test, different activated carbon loaded nano-iron materials were prepared. They were added into different 250 mL conical flasks, and at the same time 200 mL of 4-nitrophenol with an initial concentration of 50 mg/L was added. The mixture was sealed with a silica gel plug without pH adjustment. The mixture was oscillated in a constant temperature oscillating shaker at 120 r/min. After reacting for 3 h, the water sample was taken out to rapidly analyze the concentration of 4-nitrophenol. The absorbance before and after the reaction was measured at 319 nm with an ultraviolet spectrophotometer, and the corresponding removal rate was calculated.

3. Results and discussion

3.1. Selection of factors and test plan

Factors that have great influence on the preparation of nano-iron are selected: $FeSO_4$ and $NaBH_4$ concentrations, and the dosage of activated carbon as the main investigation factors [9, 10], denoted by X_1, X_2, and X_3, respectively, and −1, 0, and 1, respectively, represent the low, medium, and high levels of independent variables. The removal rate of 4-nitrophenol by activated carbon loaded nano-iron was taken as the response value (Y). The coding and level of experimental design factors are shown in Table 1.

3.2. Establishment of model equation and significance test

According to Box-Behnken's central composite experimental design, the removal rate of 4-nitrophenol by activated carbon loaded with nano-iron under different conditions is shown in Table 2.

Table 1. Level of design experimental factors

Factor	Unit	Coding	Values at each level		
			−1	0	1
$FeSO_4$	g	X_1	1	2	3
$NaBH_4$	mol/L	X_2	0.35	0.45	0.55
Activated carbon	g	X_3	4	5	6

Using Design expert 10.0 software, the removal rate test data of 4-nitrophenol in Table 2 are subjected to multiple regression fitting to obtain a quadratic multiple regression equation (1) of the removal rate and the coding independent variable, and the regression coefficient in the regression equation is estimated at the same time. The results are shown in Fig. 1 and Table 3.

$$R = 96.66 + 5.34X_1 - 0.64X_2 + 1.05X_3 + 2.85X_1X_2 - 0.77X_1X_3 - 0.23X_2X_3 - 8.28X_1^2 - 1.18X_2^2 - 2.11X_3^2 \quad (1)$$

As can be seen from Fig. 1 and Table 3, the determination coefficient of the regression model is $R2 = 0.9375$, which indicates that the fitting degree of the model is good. The model can be used to analyze and predict the removal of 4-nitrophenol by activated carbon loaded nano-iron.

3.3. Response surface analysis of removal rate 4-nitrophenol

Using Design expert 10.0 software to fit the data in Table 2, the response surface and contour lines of the obtained quadratic regression equation are shown in Fig. 2 – Fig. 4. According to the response surface and its corresponding contour map, the interaction of test factors on 4-nitrophenol removal rate can be evaluated, and the optimal horizontal range of each factor can be determined. Contour shape can reflect the intensity of interaction effect. Ellipse indicates that the interaction between the two factors is significant, while circle indicates that the interaction between the two factors is not significant [11,12].

As can be seen from Fig. 2, the interaction between the dosage of $FeSO_4$ and the concentration of $NaBH_4$ has a significant effect on the removal rate of 4-nitrophenol ($p = 0.0491 < 0.05$), which plays a key role in the performance of the prepared activated carbon loaded nano-iron material, and

Table 2. Test design and response value

Test number	Coding variable level			Removal rate of 4-nitrophenol, %
	X_1	X_2	X_3	
1	−1	0	1	80.3
2	1	0	1	92.9
3	1	1	0	91.8
4	0	0	0	96.3
5	0	−1	1	94.8
6	0	0	0	96.9
7	−1	0	−1	78.1
8	0	0	0	96.8
9	1	−1	0	89.8
10	0	1	1	95.5
11	0	0	0	96.6
12	−1	1	0	78.9
13	1	0	−1	93.8
14	0	−1	−1	90.8
15	−1	−1	0	88.3
16	0	0	0	96.4
17	0	1	−1	92.4

the concentration change of $FeSO_4$ plays an important role in the performance of the nano-iron material.

From Fig. 3, it can be seen that the interaction between the dosage of $FeSO_4$ and the dosage of activated carbon also has a significant effect on the removal rate of 4-nitrophenol, but from the slope of the dosage surface of $FeSO_4$ is larger than that of the dosage surface of activated carbon, it can be seen that the effect of the dosage of activated carbon on the removal rate of 4-nitrophenol is larger than that of the concentration of $FeSO_4$ on 4-nitrophenol.

From Fig. 4, it can be seen that the interaction between activated carbon dosage and concentration has no significant effect on the removal rate of 4-nitrophenol, but the effect of activated carbon dosage is more significant than concentration.

By solving the regression model Y, it is concluded that the removal rate of 4-nitrophenol is the target pollutant, and the optimal preparation process conditions of activated carbon loaded with nano-iron are 2.334 g of solution 100 mL, 0.462 mol/L of $NaBH_4$ solution 50 mL, and the dosage of activated carbon 5.182 g. Under these conditions, the maximum removal rate of 4-nitrophenol is predicted by the equation to be 97.6 %.

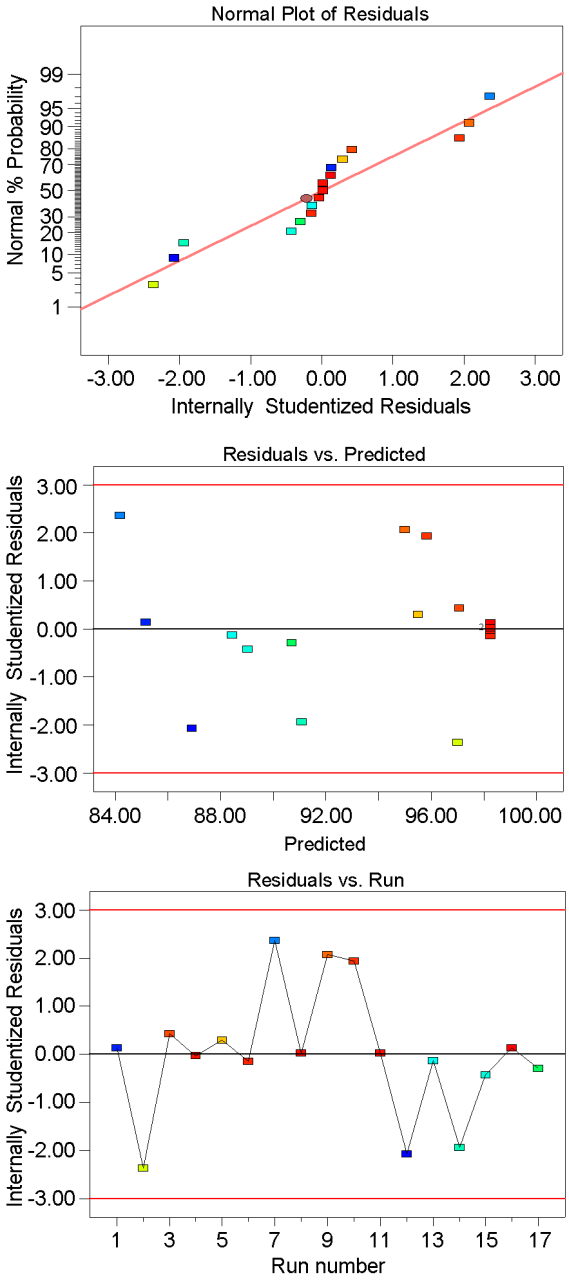

Fig. 1. Residual plot of removal rate.

3.4. Verification experiment

Under the optimal process conditions, the prepared activated carbon loaded nano-iron material was tested for its removal rate of 4-nitrophenol as shown in Fig. 5. When activated carbon and activated carbon loaded nano-iron materials are added, the removal rate of 4-nitrophenol gradually increases with the extension of reaction time. The removal rates of 4-nitrophenol were 56.5 % and 98.2 % respectively at 3 h. The activated carbon loaded nano-iron material organically combines the advantages of activated carbon

Table 3. Coefficient of regression equation and significance test

Source	Sum of squares	Variance	Mean square	*F*	*P*
Model	804.08	9	67.12	11.67	0.0019
X_1	227.91	1	227.91	39.62	0.0004
X_2	3.25	1	3.25	0.57	0.4767
X_3	8.82	1	8.82	1.53	0.2555
X_1X_2	32.49	1	32.49	5.65	0.0491
X_1X_3	2.40	1	2.40	0.42	0.5007
X_2X_3	0.20	1	0.20	0.035	0.8565
X_1^2	288.67	1	288.67	50.18	0.0002
X_2^2	5.86	1	5.86	1.02	0.3463
X_3^2	18.66	1	18.66	3.24	0.1147
Residual	40.27	7	5.75		
Missing items	40.12	3	13.37	351.91	<0.0001
Pure error	0.15	4	0.038		
Total	644.34	16			

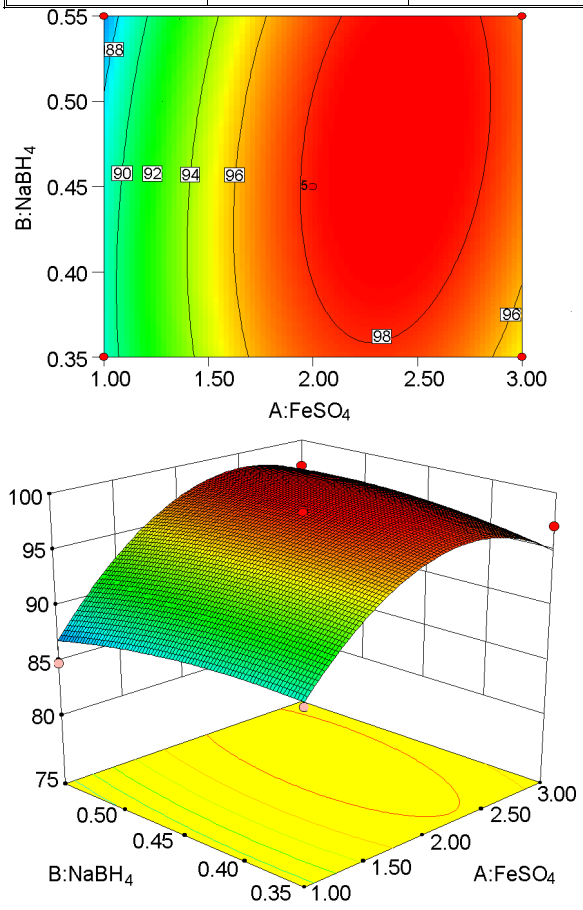

Fig. 2, Contour lines and response surfaces of $FeSO_4$ concentration and $NaBH_4$ concentration to 4-nitrophenol removal rate.

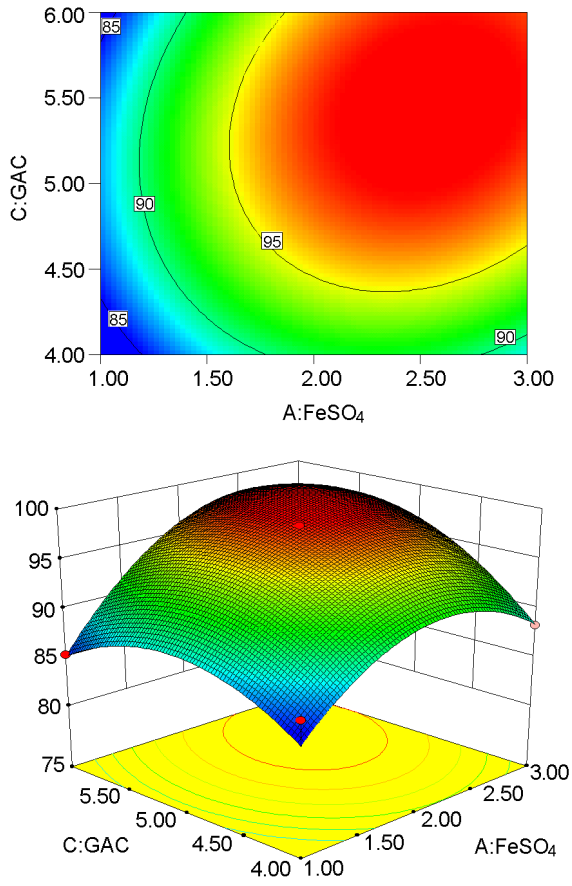

Fig. 3. Contour lines and response surfaces of active carbon dosage and $FeSO_4$ concentration on 4-nitrophenol removal rate.

and nano-iron, simultaneously exerts the adsorption effect of activated carbon and the reduction effect of nano-iron, and improves the removal effect of 4-nitrophenol. Moreover, it can exert the dispersing function of activated carbon and reduce the agglomeration of nano-iron, while the error between the removal rate obtained by the regression equation and the average value of the verification experiment is 0.4 % indicating that the prediction performance of the model is good.

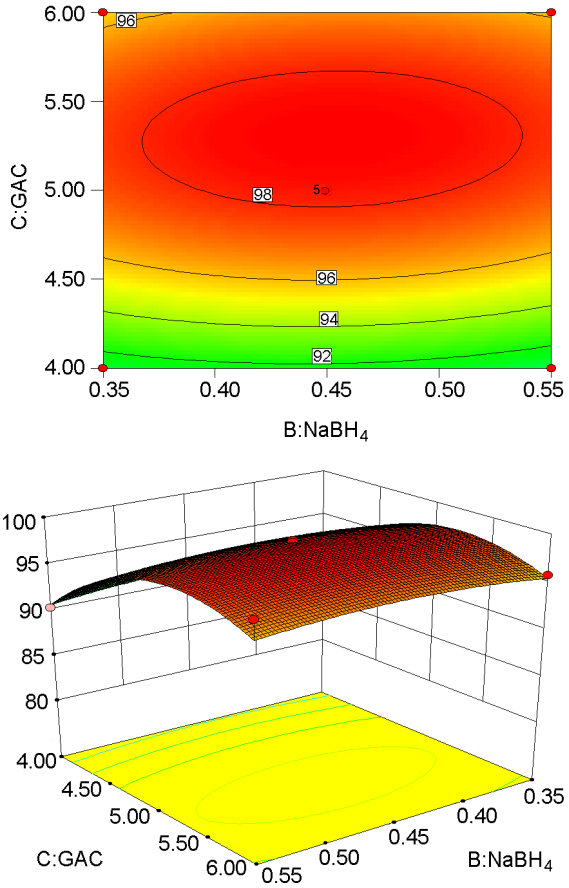

Fig. 4. Contour lines and response surfaces of activated carbon dosage and $NaBH_4$ concentration to 4-nitrophenol removal rate.

3.5. Characterization of activated carbon loaded with nano-iron

Figure 6 is an XRD diffraction pattern of activated carbon loaded nano-iron. From Fig. 5, it can be seen that some small peaks appear at $2\theta = 35 - 37°$, which are iron oxides, indicating that part of zero-valent iron loaded on activated carbon is oxidized to Fe_2O_3 and Fe_3O_4, and Fe^0 characteristic peaks [13–15] appear at $2\theta = 42 - 44°$, and the diffraction peaks are relatively weak in width and wide in dispersion, indicating that the size of loaded nano-iron particles is small.

Figure 7 is an FT-IR spectrum of activated carbon loaded nano-iron. The analysis spectrum shows that the peaks appearing at wave numbers 447.41 and 615.19 cm^{-1} are Fe–O stretching vibration peaks on Fe_2O_3 and Fe_3O_4 formed by oxidation, and the absorption peaks [16] at wave numbers 1120 cm^{-1}, 1410 cm^{-1} and 1567 cm^{-1} are all characteristic peaks corresponding to functional groups on the surface of activated carbon. The hydroxyl deformation vibration peak at wave numbers 802.25 and 1342.2 cm^{-1} is caused by hydroxyl deformation vibration in ferric hydroxide formed in the preparation process of the material, and the loaded nano-iron material has little influence on the surface functional groups of activated carbon.

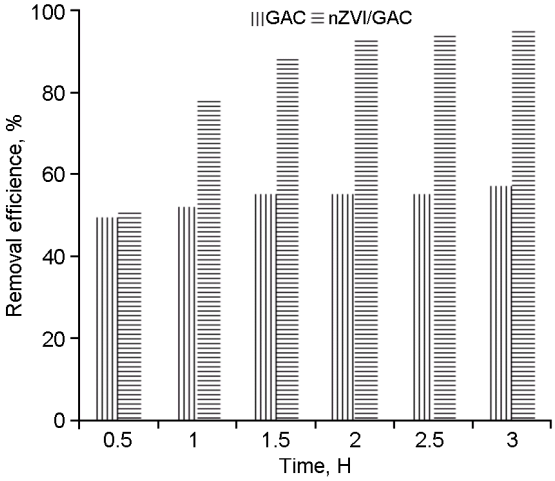

Fig. 5. Removal effect of activated carbon and activated carbon supported nano-iron on 4-nitrophenol.

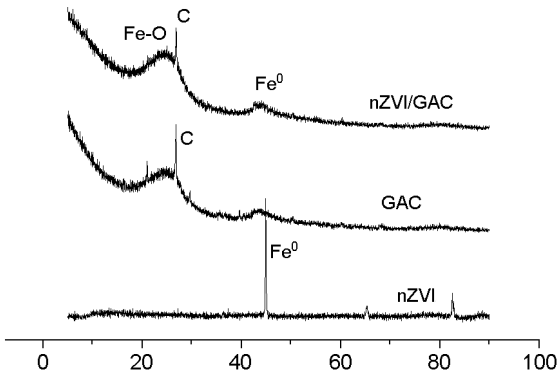

Fig. 6. XRD pattern of activated carbon supported nano-iron.

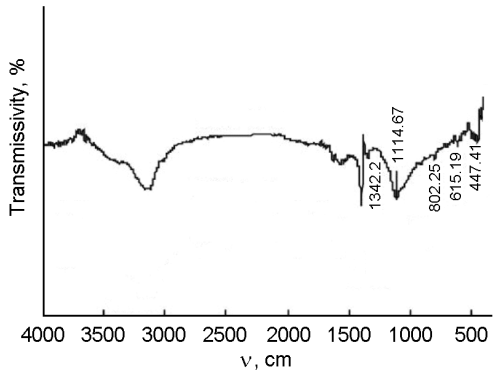

Fig. 7. FT-IR spectrum of activated carbon.

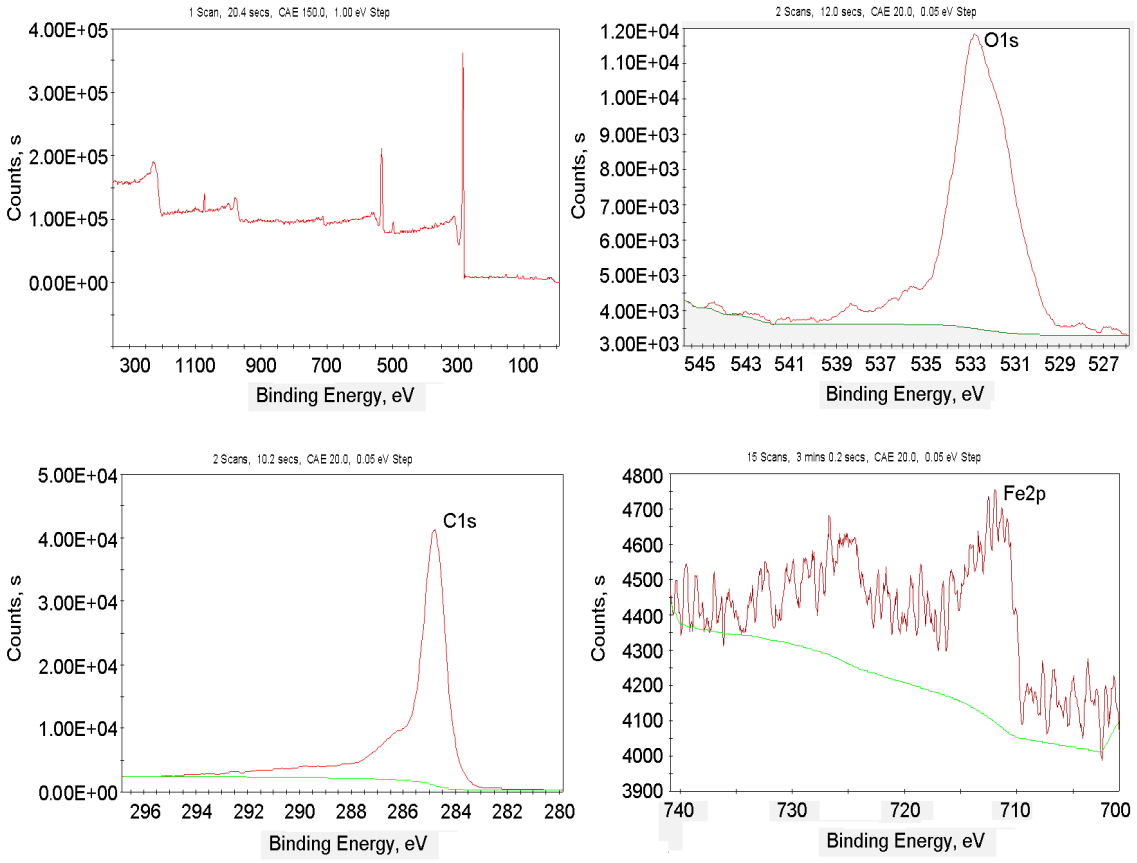

Fig. 8. XPS map of nzvi/GAC.

Table 4. Specific surface area and pore diameter of materials

Material	Specific surface area (m^2/g)	Aperture (nm)
Activated carbon	961.85	2.35
Activated carbon supports nano-iron	807.58	2.26

The XPS spectrum of nZVI/GAC material is shown in Fig. 8. Through the full spectrum scanning diagram of the material, characteristic peaks such as C, Fe and O can be seen, which indicates that the surface of the material is mainly composed of these three elements. The peak value is at 533 eV, mainly Fe_2O_3 is formed, and the spectrum range is 529.5 eV to 535.5 eV, mainly the binding energy of O2–, OH and adsorbed water molecules. There are two large peaks at 711.82 eV and 725 eV, respectively, which are mainly oxides of ferrous and ferric iron. This is due to the oxidation of zero-valent iron in the air of the prepared nZVI/GAC.

Table 4 shows the specific surface area and pore diameter of activated carbon and nano-iron loaded on activated carbon. It can be seen that the specific surface area measured after the activated carbon is loaded with nano-zero valent iron is greatly reduced, reducing 614 m^2/g. The factors causing the decrease of specific surface area are: first, the specific surface area of nano zero-valent iron is much smaller than that of activated carbon, and the former reduces the overall specific surface area [7] after being loaded on activated carbon; secondly, in the process of loading activated carbon with nano zero-valent iron, nano-iron fills the pores of activated carbon, reducing the specific surface area of activated carbon by [17]. The pore size of activated carbon before and after loading nano zero-valent iron decreased from 5.22 nm before loading to 2.23 nm, which can also prove that nano zero-valent iron filled into the pores of activated carbon during loading.

4. Conclusions

Box-Behnken response surface analysis was used to optimize the preparation conditions of activated carbon loaded nano-iron

with 4-nitrophenol as the target pollutant: 2.334 g of solution 100 mL, 0.462 mol/L of $FeSO_4$ solution 50 mL, and the dosage of activated carbon 5.182 g.

The interaction between $FeSO_4$ concentration and $NaBH_4$ concentration has a significant effect on the removal of 4-nitrophenol by activated carbon loaded nano-iron materials, and the effect of concentration is more significant. The interaction between activated carbon dosage and $NaBH_4$ concentration also has a significant effect on the removal rate of 4-nitrophenol, but the effect of activated carbon dosage is more significant than $NaBH_4$ concentration.

Under the optimal process conditions, the prepared activated carbon loaded with nano-iron treated 4-nitrophenol for 3 hours, and the removal rate of nitrophenol reached 98.2 %.

Through the characterization of activated carbon supported nano-iron, the XRD pattern shows Fe^0 characteristic peak at $2\theta = 42 - 44°$. The introduction of activated carbon inhibited the contact and growth of iron nanoparticles to a certain extent and improved the dispersibility of iron nanoparticles, thus increasing the specific surface area and active sites of zero-valent iron. However, the specific surface area of activated carbon after loading nano-iron decreased 154.27 m^2/g, and the pore diameter decreased from 2.35 nm before loading to 2.26 nm after loading.

Acknowledgements. The research for this thesis is supported under Natural Science Foundation of Colleges and Universities of Jiangsu Province (Grant: 18KJD610004), the key development program supported by the Xuzhou Institute of Technology (XKY20130 06), sponsored by Qing Lan Project of Jiangsu Province, supported by Key Laboratory of Jiangxi Province for Persistant Pollutants Control and Resources Recycle, supported by Jiangsu Key Laboratory of Industrial Pollution Control a nd Resource Reuse.

References

1. A.Li, C.Tai, Z.Zhao et al., *Environmental Science & Technology*, **41**, 6841 (2007).
2. L.M.Yang, Z.L.Chen, D.Cui et al., *Chem. Eng. J.*, **359**, 894 (2019).
3. J.Feng, B.-W.Zhu, T.-T.Lim, *Chemosphere*, **73**, 1817 (2008).
4. L.N.Shi, X.Zhang, Z.L.Chen, *Water Res.*, **45**, 886 (2011).
5. Q.Du, S.Zhang, B.Pan et al., *Water Res.*, **47**, 6064 (2013).
6. Y.-F.Su, Y.-I.Cheng, Y.-H.Shih, *J. Environ. Manag.*, **129**, 361 (2013).
7. X.Ling, J.Li, W.Zhu et al., *Chemosphere*, **87**, 655 (2012).
8. X.Wang, J.Yang, M.Zhu, F.Li, *J. Taiwan Inst. Chem. Eng.*, **44**, 386 (2013).
9. M.Kallel, C.Belaid, T.Mechichi, *Chem. Eng. J.*, **150**, 391 (2009).
10. R.Tabaraki, E.Heidarizadi, A.Benvidi, *Sep. Purif. Technol.*, **98**, 16 (2012).
11. M.T.Izquierdo, A.M.de Yuso, R.Valenciano et al., *Appl. Surf. Sci.*, **264**, 335 (2013).
12. S.D.Priyadharshini, A.K.Bakthavatsalam, *Bioresource Technology*, **207**, 150 (2016).
13. B.Y.Tak, B.S.Tak, Y.J.Kim et al., *J. Industr. Engin. Chem.*, **28**, 307 (2015).
14. S.S.Khaloo, S.Fattahi, *Desalin. Water Treat.*, **52**, 3403 (2014).
15. R.Mukherjee, R.Kumar, A.Sinha et al., *Crit. Rev. Environ. Sci. Technol.*, **46**, 443 (2016).
16. S.Hu, H.Yao, K.Wang et al., *Water Air Soil Pollut.*, **2015**, 1 (2015).
17. P.Singh, P.Raizada, S.Kumari et al., *Appl. Catalysis A: General*, **476**, 9 (2014).